materials proceedings

MDPI

Proceeding Paper

Influence of Chloride and Sulphate Ions on the Electrochemical Behaviour of High-Carbon Steel in Highly Alkaline Media †

Meyssoune Meriem [1,*], Mohamed Chairi [2] and Edoardo Proverbio [2]

[1] National Higher School of Technology and Engineering, Department of Mining, Metallurgy and Materials Engineering, Annaba 23005, Algeria
[2] Department of Engineering, University of Messina, Contrada di Dio, 98168 Messina, Italy; mohamed.chairi@unime.it (M.C.); eproverbio@unime.it (E.P.)
* Correspondence: m.meyssoune@etu.ensti-annaba.dz
† Presented at the 3rd International Online Conference on Corrosion and Materials Degradation, 30 June–2 July 2026; Available online: https://sciforum.net/event/CMD2026.

Abstract

The electrochemical behaviour of high-carbon steel was examined in highly alkaline simulated concrete pore solutions with varying chloride and sulphate concentrations. Electrochemical measurements, including open-circuit potential (OCP), electrochemical impedance spectroscopy (EIS), and potentiodynamic polarization, were conducted at multiple immersion times to assess passive-film stability. Results show that at low chloride concentrations steel maintains a stable passive state, while higher chloride concentrations facilitate passive-film degradation. Sulphate ions altered this electrochemical response through competitive adsorption, affecting passive-film properties and influencing passive film breakdown. The combined influence of chloride, sulphate, and exposure duration significantly impacts corrosion behaviour, offering valuable insights into the durability of steel in concrete environments.

Keywords: high-carbon steel; corrosion; simulated concrete pore solution; passive film

1. Introduction

The wide application of prestressed concrete structures in bridges, buildings, marine constructions, and other engineering structures is related to their high performance and durability [1–3]. In this case, it should be noted that one of the main factors determining the durability of this type of structure is the steel's resistance to corrosion [4,5]. Normally, due to the highly alkaline nature of the pore solution formed during cement hydration, a passive oxide film forms on the surface of the steel, thereby preventing corrosion [6–8]. However, if aggressive ions enter the concrete, this film may be damaged, causing localised corrosion [9].

Many aggressive species can penetrate the concrete promoting corrosion of steel in reinforced and prestressed concrete structures; however, the most dangerous among them are chloride ions, which are considered the primary cause of corrosion [2,6]. These ions enter the concrete from the marine environment, de-icing salts, and contaminated raw materials. Once they reach a certain concentration, these ions destabilise the passive film, causing pitting corrosion [3,9,10].

Apart from chlorides, sulphates are another common constituent of groundwater, seawater, industrial settings, and sulphate-containing soils. While their effect on steel corrosion is not as clearly understood as that of chlorides, some authors claim that sulphates can act

Check for updates

Academic Editor: María Criado Sanz

Published: 22 October 2026

Copyright: © 2026 by the authors. Licensee MDPI, Basel, Switzerland. This article is an open access article distributed under the terms and conditions of the Creative Commons Attribution (CC BY) license.

in some cases as corrosion inhibitors stabilising passive films, by competing with chlorides for adsorption sites, thus preventing the destruction of the passive film under specific conditions [11–14]. In other studies, it was found that sulphates affect the composition of corrosion products and the electrochemical activity of steels [15]. This implies that steel corrosion in the concrete pore solution depends not only on the concentration of individual aggressive ions but also on the combined effects of all of them.

Another very important factor affecting the corrosion process is the exposure time. Despite the rapid formation of the passive film under highly alkaline conditions, its chemical composition, thickness, and protective capabilities continue to change during exposure [16–18]. Sulphate ions can further influence this evolution through their interaction with the steel surface and their competition with chloride ions, with their effect depending on the relative concentrations of both species [11].

Electrochemical methods have proven useful for studying these processes. Open Circuit Potential (OCP) is used to determine the tendency of steel to corrode; electrochemical impedance spectroscopy (EIS) is used to study the electrochemical characteristics of the passive film; and potentiodynamic polarisation studies help elucidate the kinetics of corrosion [16,19,20]. Along with that, estimation of the thickness of the passive film by means of the Hirschhorn–Orazem power law is performed.

In the present work, the effect of chloride and sulphate ions on the electrochemical behaviour of high-carbon steel in modified concrete pore solutions was studied. Four different electrolytes with varying amounts of chloride and sulphate were analysed at 0, 7, and 21 days. The electrochemical analysis was performed by OCP, EIS and potentiodynamic polarisation measurements, and the thickness of the passive film was estimated from the EIS data. The results obtained will provide new information on the influence of chloride and sulphate concentrations and exposure time on the corrosion of high-carbon steel in an alkaline environment.

2. Experimental Procedure

Commercially available hot-rolled high-carbon steel wire rod, containing 0.82 wt.% C, was used as the substrate for the present study. The chemical composition of the steel is presented in Table 1.

Table 1. Chemical composition of the hot rolled wire.

C	Mn	Si	P	S	Cr	Ni	Mo	Cu	Al	V
0.8200	0.6850	0.2460	0.0100	0.0120	0.2190	0.0510	0.0070	0.05870	0.0020	0.0480

Samples were embedded in epoxy resin, successively abraded with silicon carbide abrasive papers and subsequently polished to a mirror finish before conducting any experiments. Simulated concrete pore solution (SCPS) was prepared by dissolving 0.131 M NaOH, 0.320 M KOH, 0.0032 M $CaSO_4 \cdot 2H_2O$, and 0.032 M $Ca(OH)_2$ in deionised water, yielding a solution with a pH of around 13.5 open to air. To investigate the effect of aggressive ions on high-carbon steel in a concrete pore environment, chloride and sulphate ions were introduced into the base SCPS using NaCl as the source of Cl^- and $CaSO_4 \cdot 2H_2O$ as the source of SO_4^{2-}, respectively. The required amounts of NaCl and $CaSO_4 \cdot 2H_2O$ were added to the base SCPS before the start of the immersion experiments, and the resulting solutions were homogenised before the steel specimens were immersed. Thus, the specified chloride and sulphate concentrations were present from the beginning of immersion. The concentrations reported in Table 2 represent the additional amounts of Cl^- and SO_4^{2-} added to the base SCPS and therefore do not include the 0.0032 M SO_4^{2-} intrinsically supplied by

$CaSO_4 \cdot 2H_2O$ in the base solution. Accordingly, the total SO_4^{2-} concentration in each test solution was equal to 0.0032 M plus the corresponding additional sulphate concentration reported in Table 2. No further addition or replenishment of Cl^- or SO_4^{2-} was performed after immersion, after passivation, or at any measurement stage during the immersion period. Electrochemical analysis was carried out using the standard three-electrode system, in which the high-carbon steel sample served as the working electrode, platinum wire as the counter electrode, and Ag/AgCl (Saturated KCl) as the reference electrode. The electrochemical behaviour of high-carbon steel as influenced by different chloride and sulphate concentrations was examined in terms of the open-circuit potential (OCP) and electrochemical impedance spectroscopy (EIS) measurements at 0, 7, and 21 days of immersion. Potentiodynamic polarisation tests were performed after 21 days of immersion in the aggressive solutions. The impedance spectra were fitted using an equivalent electrical circuit to determine the electrochemical parameters, and the passive film thickness was subsequently estimated using the Hirschhorn–Orazem power-law model.

Table 2. Additional Cl^- and SO_4^{2-} concentrations added to the base SCPS for each test solution.

Solution	Cl^- Concentration (M)	SO_4^{2-} Concentration (M)
LCl–LS	0.036	0.0062
LCl–HS	0.036	0.0736
HCl–LS	0.914	0.0062
HCl–HS	0.914	0.0736

The Hirschorn–Orazem power-law model treats the passive layer as a non-uniform medium whose electrical properties vary throughout its thickness [21]. Figure 1 illustrates the equivalent electrical circuit used to fit the EIS spectra. In the present study, the inner passive-film response was considered for estimating passive-film thickness; therefore, the CPE parameters Q_3 and α_3, corresponding to the inner passive-film branch of the equivalent circuit, were used in the calculation. The passive-film thickness was calculated according to the equation reported by Ogunsanya and Hansson [21]

$$\boldsymbol{\delta = \frac{(\varepsilon \varepsilon_0)^{\alpha}}{g Q \rho_{\delta}^{1-\alpha}}} \quad (1)$$

where

$$\boldsymbol{g = 1 + 2.88(1 - \alpha)^{2.375}} \quad (2)$$

where ($\boldsymbol{\varepsilon}$) is the dielectric constant of the passive film, ($\boldsymbol{\varepsilon_0}$) is the vacuum permittivity, $\boldsymbol{\rho}$ is the passive film resistivity, and $\boldsymbol{Q3}$ and $\boldsymbol{\alpha 3}$ are the constant phase element (CPE) parameters obtained from equivalent circuit fitting (see Table 3). The values of ($\boldsymbol{\varepsilon}$ = 12 μF/m) and $\boldsymbol{\rho}$ = 450 Ω·cm [21] were adopted from the literature for the passive film thickness calculations.

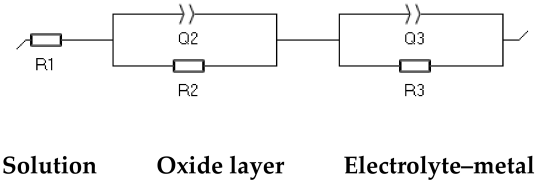


Figure 1. Equivalent electrical circuit used for fitting the EIS spectra.

Table 3. Passive film thickness at different immersion times.

Condition	Exposure Time	Q_3 ($F \cdot s^{(\alpha-1)}$)	α_3	R_3 (Ω)	δ (nm)
LCl^-/LS^-	30 min	1.948×10^{-4}	0.894	3.25×10^4	0.458
	7 d	1.608×10^{-4}	0.870	2.03×10^5	0.996
	21 d	1.66×10^{-4}	0.850	2.31×10^5	1.147
LCl^-/HS^-	30 min	2.203×10^{-4}	0.877	2.28×10^4	0.668
	7 d	1.384×10^{-4}	0.875	8.11×10^5	1.102
	21 d	2.14×10^{-4}	0.780	5.90×10^5	1.924
HCl^-/LS^-	30 min	1.957×10^{-4}	0.810	1.92×10^4	0.434
	7 d	9.879×10^{-4}	0.704	1.58×10^4	0.618
	21 d	1.99×10^{-4}	0.870	9.12×10^3	0.850
HCl^-/HS^-	30 min	2.844×10^{-4}	0.705	5.424×10^3	0.34
	7 d	2.160×10^{-4}	0.887	2.28×10^5	0.548
	21 d	3.10×10^{-4}	0.880	9.88×10^2	0.183

3. Results and Discussions

3.1. Open Circuit Potential (OCP)

The results of the 21-day open-circuit potential (OCP) testing, as presented in Figure 2, demonstrate the significant influence of chloride and sulphate ions on the corrosion stability of high-carbon steel in simulated concrete pore solutions. At day zero, after 30 min of immersion, all samples exhibited relatively negative OCP values (approximately −0.34 to −0.47 V), indicating electrochemically active surfaces with limited passive-film development. Between day zero and day seven, OCP values shifted positively in all solutions, reaching approximately −0.25 to −0.27 V, suggesting the initial formation and stabilisation of a passive oxide layer promoted by the highly alkaline environment. After day seven, a clear divergence emerged. Under high-chloride conditions, the OCP of HCl/LS decreased from −0.270 V at day 7 to −0.469 V at day 21. In comparison, HCl/HS decreased from −0.246 V to −0.460 V, indicating significant passive-film destabilisation and the development of active corrosion. The slightly less negative final potential in HCl/HS compared with HCl/LS does not indicate a protective effect of sulphate under high-chloride conditions; rather, the combined presence of high chloride and high sulphate still resulted in substantial deterioration of the passive state.

In contrast, under low-chloride conditions, OCP remained relatively stable and shifted further positive by day 21, particularly for LCl/HS, which reached −0.208 V, indicating a beneficial effect of higher sulphate concentration under low-chloride conditions. This observation is consistent with the findings of Liu, Lupeng et al. [10,22], who reported that OCP progressively increases with immersion time when the chloride concentration remains below the threshold. In contrast, at concentrations above the threshold, OCP initially increases before decreasing as passive-film breakdown occurs. According to ASTM C876, active steel corrosion is less than 10% probable for potentials more positive than −245 mV versus SCE. In contrast, potentials more negative than −395 mV indicate a high probability of active corrosion. Accordingly, the low-chloride conditions remained within the range associated with a stable passive state, while the high-chloride conditions reached potentials characteristic of active corrosion. Overall, the OCP evolution demonstrates that chloride concentration is the dominant factor controlling passive-film stability, while the effect of sulphate depends strongly on the chloride level [23–25].

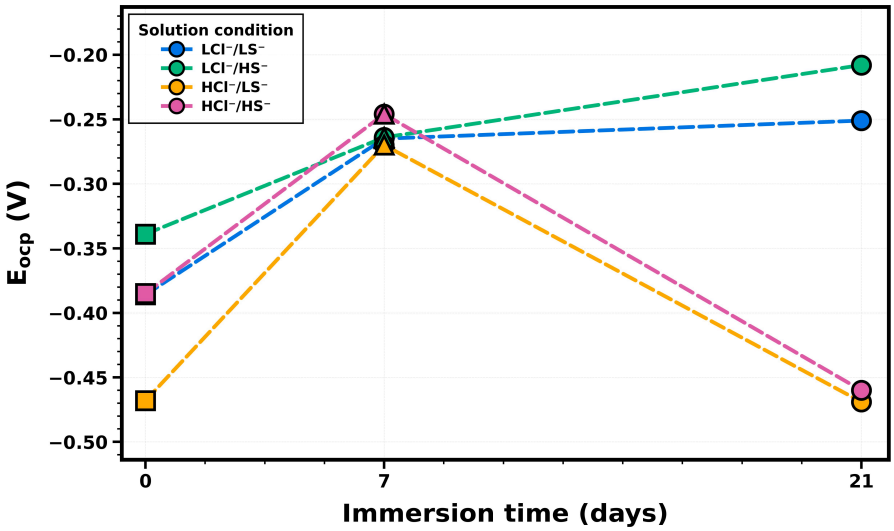


Figure 2. The evolution of Eocp with exposure time of high-carbon steel in simulated concrete pore solution with different chloride and sulphate concentrations.

3.2. Electrochemical Impedance Spectroscopy (EIS) Response

Electrochemical impedance spectra of the high-carbon steel in the modified simulated concrete pore solutions were investigated using Nyquist diagrams, which are shown in Figure 3. below. The impedance diagram displays two reduced capacitive arcs, suggesting two electrochemical time constants associated with the passive film and the charge-transfer mechanism at the steel/electrolyte contact surface [26]. The high-frequency reduced capacitive arc suggests the contributions of the passive film's resistance and capacitance, while the low-frequency reduced capacitive arc relates to charge transfer in the corrosion process. At the initial immersion time (0 days), there were small diameter arcs, suggesting that there was low polarisation resistance and a thin passive film formed. This observation is consistent with the negative value of the OCP at the early stage of the immersion test period.

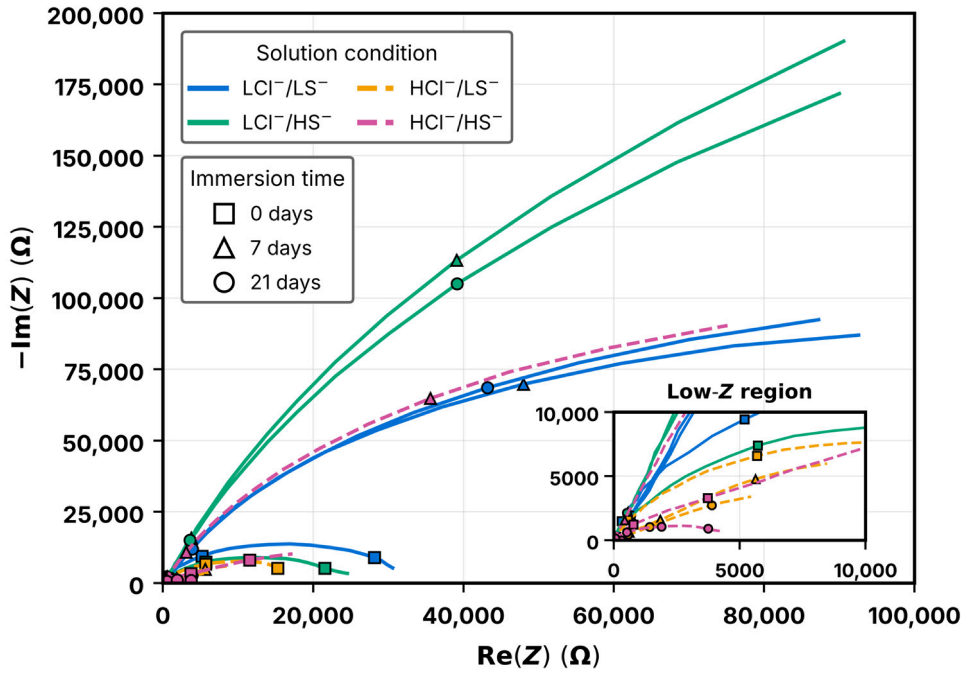


Figure 3. Nyquist plots of EIS measurements for low- and high-chloride/sulphate environments at different immersion times.

After 7 days of immersion in low-chloride media, the impedance response of the samples increased significantly, indicating the gradual formation of a protective passive film. This result corresponds to a cathodic shift in OCP values and implies improved corrosion resistance. However, the impedance changes were lower in high-chloride solutions, which may indicate the onset of chloride interference during passive film formation.

After 21 days of immersion, there was an even more noticeable difference between these conditions. The maximum value of the capacitive loop was observed under the LCl/HS condition, indicating the highest electrochemical resistance and the most developed protective passive film. On the contrary, the HCl/HS condition caused a dramatic decrease in impedance, indicating the destruction of the passive film and activation of corrosion. Although there is still a notable impedance response under this condition, it could be related to the formation of resistive corrosion products. Such results correspond to the cathodic shift in the OCP value. This behaviour can be attributed to the competition of chloride and sulphate ions on the steel surface [13]. In the initial stages of exposure, sulphate ions compete with chloride ions for adsorption sites and thus limit the degradation of the passive film due to the presence of chloride ions. As time passes, chloride ions begin to destabilise the passive film, causing its destruction and increasing the corrosion rate [21,24]. The same behaviour was observed by Ogunsanya et al. [21], in that increased chloride ions shift the corrosion potential to more negative values, while increased sulphate ions counteract this effect.

The fitting of the impedance spectra was performed using the equivalent circuit shown in Figure 1, from which R_3, representing the passive-film resistance, was obtained and considered as a key parameter for evaluating the resistance properties of the passive film (Table 3). As shown in Table 3, the increase in passive-film thickness corresponds to an increase in R_3 and a decrease in the CPE exponent α_3, indicating an increase in the non-ideal behaviour of the film as it develops. This trend was most evident when comparing the two opposite cases: LCl/HS resulted in the thickest film (1.924 nm) and the highest R_3 value (5.90×10^5 Ω), whereas HCl/HS resulted in the thinnest film (0.183 nm) and the lowest R_3 value (9.88×10^2 Ω) (Table 3). The effect of sulphate ions was therefore strongly dependent on the chloride concentration: sulphate stabilised the passive film at low chloride concentration, whereas at high chloride concentration, the combined presence of chloride and sulphate resulted in a synergistic effect that aggravated passive-film degradation, as evidenced by the reduced film thickness and R_3 value.

3.3. Anodic Polarisation

As shown in the polarisation curves (Figure 4) and the electrochemical parameters reported in Table 4, the corrosion behaviour of high-carbon steel is strongly influenced by the combined concentrations of chloride and sulphate ions. Under low-chloride conditions, increasing the sulphate concentration from LCl/LS to LCl/HS resulted in a decrease in the corrosion current density from 0.232 to 0.061 μA cm^{-2}, together with an increase in the pitting potential from 0.60 to 0.63 V, indicating enhanced passive-film stability. In contrast, under high-chloride conditions, the effect of sulphate was markedly different. Increasing the sulphate concentration from HCl/LS to HCl/HS increased the corrosion current density from 4.31 to 7.12 μA cm^{-2} and caused a pronounced decrease in the pitting potential from 0.42 to 0.026 V, indicating a higher susceptibility to passive-film breakdown and localised corrosion. Thus, sulphate ions do not exert a universally protective effect; their influence depends strongly on the chloride concentration. While sulphate can contribute to passive-film stabilisation when chloride concentration is low, at high chloride concentration its presence may enhance the deleterious effect of chloride, leading to increased corrosion activity and an earlier onset of localised corrosion. These polarisation results are consistent

with the EIS analysis, which showed the highest passive-film resistance and thickness under LCl/HS. In contrast, the HCl/HS condition exhibited the lowest passive-film resistance and thickness [11,15,27,28].

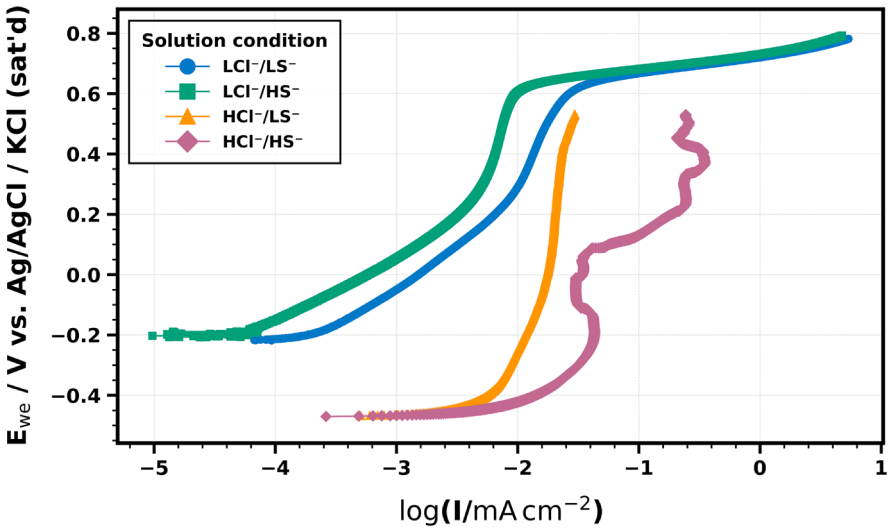


Figure 4. Anodic polarisation curves of samples exposed to low- and high-chloride/sulphate conditions after 21 days of immersion.

Table 4. Corrosion current density (i_{corr}) and pitting potential (E_{pit}) obtained from potentiodynamic polarisation measurements after 21 days of immersion.

Condition	LCl-/LS-	LCl-/HS-	HCl-/LS-	HCl-/HS-
E_{pit} (V)	0.60	0.63	0.42	0.026
I_{corr} ($\mu A \cdot cm^{-2}$)	0.232	0.061	4.31	7.12

4. Conclusions

1. The combined effects of chloride and sulphate ions strongly influence the electrochemical behaviour of high-carbon pearlitic prestressing steel. Sulphate enhances passive-film stability at low chloride concentration, whereas at high chloride concentration it promotes further degradation of the passive state.
2. The combined analysis of EIS, passive-film thickness, and anodic polarisation measurements demonstrates that passive-film stability is closely related to corrosion resistance. The low-chloride conditions, particularly LCl/HS, exhibited thicker and more resistive passive films, lower corrosion current densities, and higher pitting potentials, whereas the high-chloride conditions, particularly HCl/HS, showed severe passive-film degradation, higher corrosion current density, and lower pitting potential.
3. This work provides new insight into the corrosion behaviour of high-carbon pearlitic prestressing steel by demonstrating that the beneficial effect of sulphate is strongly dependent on chloride concentration. These findings improve understanding of corrosion mechanisms in prestressed concrete exposed to combined chloride–sulphate environments and provide useful guidance for assessing the durability of prestressing steel under aggressive service conditions.

Author Contributions: Conceptualization, M.M.; methodology, M.M.; formal analysis, M.M.; investigation, M.M.; data curation, M.M. and M.C.; visualization, M.M. and M.C.; writing—original draft preparation, M.M.; writing—review and editing, M.M., M.C. and E.P.; supervision, E.P.; resources, M.M. and E.P. All authors have read and agreed to the published version of the manuscript.

Funding: This research received no external funding.

Institutional Review Board Statement: Not applicable.

Informed Consent Statement: Not applicable.

Data Availability Statement: The original contributions presented in this study are included in the article. Further inquiries can be directed to the corresponding authors.

Conflicts of Interest: The authors declare no conflicts of interest.

References

1. Vereecken, E.; Botte, W.; Lombaert, G.; Caspeele, R. Assessment of corroded prestressed and posttensioned concrete structures: A review. *Struct. Concr.* **2021**, *22*, 2556–2580. [CrossRef]
2. Wang, L. *Strand Corrosion in Prestressed Concrete Structures*; Springer: Singapore, 2023. [CrossRef]
3. Pierott, R.M.R.; Garcia, S.; Kropf, D.; Figueiredo, K.; da Costa, B.B.F.; Amario, M.; Najjar, M.K.; Haddad, A. Predictive Analysis of Corrosion Dynamics in Prestressed Concrete Exposed to Chloride Environments. *Infrastructures* **2024**, *9*, 133. [CrossRef]
4. Messina, D.; Proverbio, E. Effect of prestressing corrosion on failure in bridges. *Struct. Concr.* **2023**, *24*, 227–238. [CrossRef]
5. Carsana, M.; Bertolini, L. Corrosion failure of post-tensioning tendons in alkaline and chloride-free segregated grout: A case study. *Struct. Infrastruct. Eng.* **2014**, *11*, 402–411. [CrossRef]
6. Goyal, A.; Pouya, H.S.; Ganjian, E.; Claisse, P. A Review of Corrosion and Protection of Steel in Concrete. *Arab. J. Sci. Eng.* **2018**, *43*, 5035–5055. [CrossRef]
7. Huet, B.; L'Hostis, V.; Miserque, F.; Idrissi, H. Electrochemical behavior of mild steel in concrete: Influence of pH and carbonate content of concrete pore solution. *Electrochim. Acta* **2005**, *51*, 172–180. [CrossRef]
8. Montemor, M.F.; Simões, A.M.P.; Ferreira, M.G.S. Analytical Characterization of the Passive Film Formed on Steel in Solutions Simulating the Concrete Interstitial Electrolyte. *Corrosion* **1998**, *54*, 347–353. [CrossRef]
9. Page, C.L.; Vennesland, Ø. Pore solution composition and chloride binding capacity of silica-fume cement pastes. *Mat. Constr.* **1983**, *16*, 19–25. [CrossRef]
10. Liu, C.; Gong, K.; Wei, W.; Wang, Y.; Xie, H.; Mao, F. Coupling Influence of pH and Cl– on the Corrosion Evolution of Passivated Q355B Steel in Simulated Concrete Pore Solution. *Langmuir* **2025**, *41*, 2458–2470. [CrossRef] [PubMed]
11. Liu, G.; Zhang, Y.; Ni, Z.; Huang, R. Corrosion behavior of steel submitted to chloride and sulphate ions in simulated concrete pore solution. *Constr. Build. Mater.* **2016**, *115*, 1–5. [CrossRef]
12. Tian, Y.; Liu, Y.; Xie, Y.-M.; Zhang, G.-Y.; Ye, H.-L.; Yan, D.-M.; Li, Y.-J.; Li, B.; Xue, H.-J.; Cai, Q. Coupled effects of chlorides and sulfates on steel reinforcement corrosion in concrete structures: A comprehensive review. *Case Stud. Constr. Mater.* **2025**, *22*, e04263. [CrossRef]
13. Gong, K.; Liu, C.; Yang, M.; Mao, F. Effect of Cl−, SO4 2−, and pH on the corrosion behaviour and depassivation mechanism of Q355B steel in simulated concrete pore solution. *J. Mater. Sci.* **2025**, *60*, 3518–3538. [CrossRef]
14. Liu, G.; Li, J.; Zhang, Y. Corrosion of carbon steels subjected to chloride and sulfate in simulated concrete pore solutions with different pH. *Constr. Build. Mater.* **2024**, *440*, 137445. [CrossRef]
15. Chen, Z.; Wang, Y.; Nong, Y.; Wei, Z.; Chen, Y. Mechanism of rebar depassivation in concrete containing sulphate: A vicious cycle between sulphate adsorption and surface vacancy formation. *Corros. Sci.* **2024**, *234*, 112126. [CrossRef]
16. Joiret, S.; Keddam, M.; Nóvoa, X.R.; Pérez, M.C.; Rangel, C.; Takenouti, H. Use of EIS, Ring-Disk Electrode, EQCM and Raman Spectroscopy to Study the Film of Oxides Formed on Iron in 1 M NaOH. *Cem. Concr. Compos.* **2002**, *24*, 7–15. [CrossRef]
17. Tang, Y.M.; Miao, Y.F.; Zuo, Y.; Zhang, G.D.; Wang, C.L. Corrosion behavior of steel in simulated concrete pore solutions treated with calcium silicate hydrates. *Constr. Build. Mater.* **2012**, *30*, 252–256. [CrossRef]
18. Liu, W.; Wang, L.; Zhou, L.; Yang, Q.; Dong, B.; Wang, X.; Hong, S. Electrochemical-structural evolution and formation mechanism of the passive film on carbon steel in simulated concrete pore solution. *Case Stud. Constr. Mater.* **2026**, *24*, e06122. [CrossRef]
19. Hansson, C.M. Comments on electrochemical measurements of the rate of corrosion of steel in concrete. *Cem. Concr. Res.* **1984**, *14*, 574–584. [CrossRef]
20. Jolivet, D.; Bonen, D.M.; Shah, S.P. The corrosion resistance of coated steel dowels determined by impedance spectroscopy. *Cem. Concr. Res.* **2007**, *37*, 1134–1143. [CrossRef]
21. Ogunsanya, I.G.; Hansson, C.M. Influence of chloride and sulphate anions on the electronic and electrochemical properties of passive films formed on steel reinforcing bars. *Materialia* **2019**, *8*, 100491. [CrossRef]
22. Liu, L.; Li, S.; Gao, Z.; Jia, H.; Hu, W. Effect of chloride concentration on the properties of passive film formed on Q235 steel in simulated concrete pore solutions. *Anti-Corros. Methods Mater.* **2023**, *70*, 9–17. [CrossRef]
23. Liu, R.; Jiang, L.; Xu, J.; Xiong, C.; Song, Z. Influence of carbonation on chloride-induced reinforcement corrosion in simulated concrete pore solutions. *Constr. Build. Mater.* **2014**, *56*, 16–20. [CrossRef]

24. Melo, P.; Echagüe, M.; Guerra, C.; Jin, Q.; Sancy, M.; Paul, A. On the effect of simulated contamination of chlorides and sulfates on steel rebar corrosion: Electrochemical behavior and surface analysis. *Constr. Build. Mater.* **2022**, *359*, 129337. [CrossRef]
25. DorMohammadi, H.; Pang, Q.; Murkute, P.; Árnadóttir, L.; Isgor, O.B. Investigation of chloride-induced depassivation of iron in alkaline media by reactive force field molecular dynamics. *npj Mater. Degrad.* **2019**, *3*, 19. [CrossRef]
26. Jin, Z.; Zhao, X.; Du, Y.; Yang, S.; Wang, D.; Zhao, T.; Bai, Y. Comprehensive properties of passive film formed in simulated pore solution of alkali-activated concrete. *Constr. Build. Mater.* **2022**, *319*, 126142. [CrossRef]
27. Liu, C.; Mao, F.; Wang, J.; Li, B. Combined effect of chloride and sulfate ions on the corrosion behavior of Q355B steel in simulated concrete pore solution. *Mater. Today Commun.* **2024**, *40*, 109703. [CrossRef]
28. Pradhan, B. Corrosion behavior of steel reinforcement in concrete exposed to composite chloride-sulfate environment. *Constr. Build. Mater.* **2014**, *72*, 398–410. [CrossRef]

Disclaimer/Publisher's Note: The statements, opinions and data contained in all publications are solely those of the individual author(s) and contributor(s) and not of MDPI and/or the editor(s). MDPI and/or the editor(s) disclaim responsibility for any injury to people or property resulting from any ideas, methods, instructions or products referred to in the content.